The Journal of Immunology

RESEARCH ARTICLE | JANUARY 01 2008

Chemokine Receptor CX3CR1 Mediates Skin Wound Healing by Promoting Macrophage and Fibroblast Accumulation and Function[1] FREE

Yuko Ishida; ... et. al

J Immunol (2008) 180 (1): 569–579.
https://doi.org/10.4049/jimmunol.180.1.569

Chemokine Receptor CX3CR1 Mediates Skin Wound Healing by Promoting Macrophage and Fibroblast Accumulation and Function[1]

Yuko Ishida, Ji-Liang Gao, and Philip M. Murphy[2]

Wounds heal through a highly regulated, self-limited inflammatory response, however, precise inflammatory mediators have not been fully delineated. In this study, we report that in a mouse model of excisional skin wound healing the chemokine CX3CL1 and its receptor CX3CR1 were both highly induced at wound sites; CX3CL1 colocalized with macrophages and endothelial cells, whereas CX3CR1 colocalized mainly with macrophages and fibroblasts. Loss of CX3CR1 function delayed wound closure in both CX3CR1 knockout (KO) mice and in wild-type mice infused with anti-CX3CR1-neutralizing Ab. Conversely, transfer of bone marrow from donor wild-type mice, but not from donor CX3CR1 KO mice, restored wound healing to normal in CX3CR1 KO-recipient mice. Direct effects of CX3CR1 disruption at the wound site included marked reduction of macrophages and macrophage products, such as TGF-β1 and vascular endothelial growth factor. Consistent with this, we observed reduced α-smooth muscle actin (a marker for myofibroblasts) and collagen deposition in skin from wounded CX3CR1 KO mice, as well as reduced neovascularization. Together, the data support a molecular model of skin wound repair in which CX3CR1 mediates direct recruitment of bone marrow-derived monocytes/macrophages which release profibrotic and angiogenic mediators. ***The Journal of Immunology,*** **2008, 180: 569–579.**

Repair of tissue damage is an interactive process that involves soluble mediators, extracellular matrix components, resident cells, and infiltrating leukocytes, which participate differentially in three sequential phases: inflammation, proliferation, and maturation (1). Initially, neutrophils accumulate in wound sites, followed by a large influx of macrophages and a small number of T lymphocytes. In the proliferative phase, massive angiogenesis occurs, and fibroblasts migrate into the wound, proliferate, and transform into myofibroblasts, which play a major role in granulation tissue formation. The molecular mediators of wound repair are not fully understood but include cytokines, chemokines, matrix proteins, matrix metalloproteinases, and growth factors (2–6). This article is focused on the chemokines, a major class of leukocyte chemoattractant proteins, which can be classified into four distinct groups, named C, CC, CXC, and CX3C, based on patterns of conserved cysteines. The chemokines MCP-1/CCL2, MIP-1α/CCL3, and IFN-γ-inducible protein 10/CXCL10, and the chemokine receptor CXCR2 have been identified as regulators of specific leukocyte accumulation at wound sites (3, 7–11). However, the involvement of most chemokines in wound healing has not yet been addressed. We surveyed expression of inflammatory chemokines in a mouse model of skin wound healing to begin to fill this gap. In so doing, we identified particularly high expression of CX3CL1 (also known as fractalkine), the only known member of the CX3C chemokine subfamily, and its receptor CX3CR1.

CX3CL1 is expressed as a soluble chemokine domain form and as a membrane-bound form on the surface of inflamed endothelial cells, epithelial cells, macrophages, and vascular smooth muscle cells. Interaction between membrane-bound CX3CL1 and CX3CR1 on leukocytes mediates cell-cell adhesion (12–14). CX3CL1 is expressed in various organs, including skin. CX3CR1 is expressed by monocytes/macrophages, NK cells, a subpopulation of T cells, and smooth muscle cells (14–18). Accumulating evidence suggests that CX3CL1-CX3CR1 interaction contributes to the development of inflammatory diseases, such as rheumatoid arthritis, glomerulonephritis, atopic dermatitis, psoriasis, Crohn's disease, and atherosclerosis (15, 19–23).

Chemokines and their receptors not only may coordinate leukocyte infiltration but also may modulate the function of nonhemopoietic and resident cells in damaged tissue, both directly and indirectly (2, 3). Recently, a profibrotic activity has been suggested for CX3CL1/CX3CR1 based on the finding that patients with systemic sclerosis have increased expression of CX3CL1 and increased CX3CR1$^+$ leukocytes in fibrotic skin and lung lesions (16). Moreover, bone marrow (BM)[3] cells are known to play important roles in multiple organs in repair/regeneration of injured tissues, through a complex interplay between adhesion molecules, cytokines, and chemokines (3, 24, 25), and CX3CR1 is expressed on most monocytes/macrophages (16–18, 21, 23). Based on this information, we hypothesized that CX3CL1-CX3CR1 may have multiple roles in wound healing. In the present study, we tested this hypothesis in a mouse model of excisional skin wound healing.

Molecular Signaling Section, Laboratory of Molecular Immunology, National Institute of Allergy and Infectious Diseases, National Institutes of Health, Bethesda, MD 20892

Received for publication September 7, 2007. Accepted for publication October 20, 2007.

The costs of publication of this article were defrayed in part by the payment of page charges. This article must therefore be hereby marked *advertisement* in accordance with 18 U.S.C. Section 1734 solely to indicate this fact.

[1] This work was supported by the Intramural Research Program of the National Institute of Allergy and Infectious Diseases.

[2] Address correspondence and reprint requests to Dr. Philip M. Murphy, Molecular Signaling Section, Laboratory of Molecular Immunology, National Institute of Allergy and Infectious Diseases, National Institutes of Health, 9000 Rockville Pike, Building 10, Room 11N113, Bethesda, MD 20892. E-mail address: pmm@nih.gov

[3] Abbreviations used in this paper: BM, bone marrow; pAb, polyclonal Ab; MPO, myeloperoxidase; α-SMA, α-smooth muscle actin; KO, knockout; WT, wild type; VEGF, vascular endothelial growth factor; AMCA, aminomethylcoumarin acetate.

Materials and Methods

Antibodies

The following mAbs and polyclonal Abs (pAbs) were used in this study: rabbit anti-myeloperoxidase (MPO) pAb (Lab Vision), which reacts with mouse MPO; rat anti-mouse CD31 mAb (BD Biosciences); rat anti-mouse F4/80 mAb (clone BM8; eBioscience); rabbit anti-human CD3 pAb (DakoCytomation), which cross-reacts with mouse CD3; mouse anti-human α-smooth muscle actin (α-SMA) mAb (clone 1A4; DakoCytomation), which cross-reacts with mouse α-SMA; rabbit anti-CX3CR1 pAb (Abcam), which reacts with mouse CX3CR1; goat anti-mouse CCR2 pAb (Abcam); goat anti-mouse CX3CL1 pAb (R&D Systems); cyanine dye 3 (Cy3)-conjugated donkey anti-rat, -mouse, and -goat IgG, FITC-conjugated donkey anti-rabbit and anti-goat IgG, and aminomethylcoumarin acetate (AMCA)-conjugated donkey anti-rat IgG pAbs (Jackson ImmunoResearch Laboratories); and rabbit anti-CX3CR1-neutralizing pAb and control rabbit IgG (Torrey Pines Biolabs).

Animals

Male CX3CR1 knockout (KO) mice, generated as previously described (26), were backcrossed onto C57BL/6 mice from Taconic Farms for 10 generations. Control C57BL/6 mice were obtained from Taconic Farms. All animals were used at 8–10 wk of age and housed individually in cages under specific pathogen-free conditions during the experiments. All animals were used under the auspices of a protocol approved by the National Institute of Allergy and Infectious Diseases Animal Care and Use Committee.

Excisional wound preparation and analysis

Full-thickness wounds were created in the dorsal skin under sterile conditions. Briefly, mice were anesthetized with i.p. administration of ketamine and xylazine. After shaving and cleaning with betadine and 70% ethanol, the dorsal skin was picked up at the midline and punched through two layers of skin with a sterile disposable biopsy punch (4 mm in diameter; Miltex), generating one wound on each side of the midline. The same procedure was repeated three times, generating six wounds. Each wound site was digitally photographed at the indicated time intervals, and wound areas were determined on photographs using Adobe PhotoShop (version 7.0; Adobe Systems). Changes in wound areas over time were expressed as the percentage of the initial wound areas. In another series of experiments, 100 μl of anti-CX3CR1-neutralizing pAb or control IgG was administered i.p. at a concentration of 20 μg/ml into wild-type (WT) mice immediately after wounding as described previously (18, 27, 28). Thereafter, animals received similar injections each day up to 5 days following wound preparation. In some experiments, wounds and their surrounding areas, including the scab and epithelial margins, were cut at the indicated time intervals with a sterile disposable 8-mm diameter biopsy punch.

Histopathological analysis of wound sites

Wound specimens were fixed in 4% formaldehyde buffered with PBS and then embedded with paraffin. Sections were stained with H&E for histological analysis. Immunohistochemical analyses were also performed using anti-MPO, -F4/80, -CD3, -CD31, -α-SMA, -CX3CR1, or -CX3CL1 Abs, as described previously (5, 29). Deparaffinized sections were immersed in 0.3% H_2O_2 in methanol for 30 min to eliminate endogenous peroxidase activities. The sections were further incubated with PBS containing 1% normal serum corresponding to the secondary Ab and 1% BSA to reduce nonspecific reactions. The sections were incubated with Abs at a concentration of 1 μg/ml at 4°C overnight. Normal rat, rabbit, goat, or mouse IgG was used as negative control. After incubation with biotinylated secondary Ab, immune complexes were visualized using the Catalyzed Signal Amplification System (DakoCytomation) according to the manufacturer's instructions.

Immunofluorescence microscopy

Wound sections were also analyzed by double- or triple-color immunofluorescence microscopy to determine the localization of CX3CL1, CX3CR1, and CCR2 proteins as described previously (30, 31). Briefly, deparaffinized sections were incubated with PBS containing 1% normal donkey serum and 1% BSA to reduce nonspecific reactions. Then, the sections were further incubated with the combination of anti-CX3CR1 and -F4/80, anti-α-SMA or -CD31; anti-CX3CL1 and -F4/80; and anti-F4/80, -CX3CR1, and -CCR2 Abs at 4°C overnight. All Abs were used at a concentration of 1 μg/ml. After incubation with fluorochrome-conjugated secondary Abs (10 μg/ml) at room temperature for 30 min, the sections were observed by fluorescence microscopy.

Measurement of leukocyte recruitment and angiogenesis at wound sites

The wound bed was defined as the area surrounded by uninjured skin and fascia, regenerated epidermis, and eschar (5, 30). The numbers of infiltrating macrophages and T cells within the wound beds were enumerated on 10 randomly chosen visual fields ($\times$200) of the sections stained with anti-F4/80 and -CD3 Ab, respectively, and the average of the selected 10 fields was calculated. Using the freehand tool of PhotoShop, vascular areas, defined as CD31 immunoreactive in the wound beds, were measured and were expressed as the percentage of the entire wound bed area. All sample identifiers were blinded to the observer.

MPO assay

MPO activity was measured to evaluate neutrophil recruitment (5, 30). Skin wound sites were excised using a sterile disposable 8-mm diameter biopsy punch and were then homogenized in 1 ml of 50 mM potassium phosphate buffer solution with 0.5% hexadecyltrimethylammonium bromide (Sigma-Aldrich) and 5 mM EDTA. The samples were freeze-thawed three times and centrifuged at 12,000 $\times$ *g* at 4°C. MPO activities in the supernatants were assayed using the SUMILON peroxidase assay kit (Sumitomo Bekuraito) according to the manufacturer's instructions. Absorbance was measured at 490 nm and MPO content was determined against a standard curve generated using known concentrations of reagent MPO (Sigma-Aldrich). The data were expressed as units per wound.

Measurement of hydroxyproline content

Hydroxyproline content was measured as the index of collagen accumulation at the wound sites, as described previously (5, 30). The excised wound samples were dried for 16 h at 120°C and were then hydrolyzed in 6 N HCl at 110°C for 12 h. Fifty-microliter aliquots were added to 1 ml of a solution containing 1.4% chloramine T (Sigma-Aldrich), 10% *n*-propanol, and 0.5 M sodium acetate at pH 6.0. After 20-min incubation at room temperature, 1 ml of Ehrlich's solution (1 M *p*-dimethylaminobenzaldehyde in 70% *n*-propanol, 20% perchloric acid) was added and the mixture was incubated at 65°C for 15 min. Absorbance was measured at 550 nm and the amount of hydroxyproline was determined against a standard curve generated using known concentrations of reagent hydroxyproline (Sigma-Aldrich). The data were expressed as amount (micrograms) per wound.

ELISA

Wound samples were homogenized with PBS containing Complete Protease Inhibitor Cocktail (Roche Diagnostics) and centrifuged at 5000 $\times$ *g* for 10 min. Supernatants were used to determine TGF-β1 and vascular endothelial growth factor (VEGF) levels with commercial ELISA kits (R&D Systems) according to the manufacturer's instructions. Total protein in the supernatants was measured with a commercial kit (Bicinchoninic Acid Protein Assay kit; Pierce). The data were expressed as the target molecule (picograms) per total protein (milligrams) for each sample.

Extraction of total RNAs and RT-PCR

Total RNA was isolated from uninjured and wounded skin samples using TRIzol (Invitrogen Life Technologies) reagent according to the manufacturer's instructions. Before reverse transcription, RNA was treated with RNase-free DNase I following the manufacturer's protocol. Three micrograms of total RNA was used for the synthesis of cDNA using a Superscript III RT kit (Invitrogen Life Technologies). Unique primer sets for mouse β-actin, chemokines, chemokine receptors, growth factors, and collagen type I were designed (Table I), based on sequences deposited with the National Center for Biotechnology Information, and were synthesized by Invitrogen Life Technologies. PCR was performed using 1 μl of cDNA in a reaction mix with *Taq* polymerase (Invitrogen Life Technologies). PCR was found to be linear between 20 and 35 cycles, and PCR conditions were optimized to allow for semiquantitative comparison of the results. Digital images of bands separated on ethidium bromide-stained agarose gels were quantitated using NIH Image Analysis Software. The intensity of each primer product was normalized to the intensity of the β-actin primer product, and expressed relative to the levels found in uninjured skin of WT mice.

Generation of BM chimera mice

The protocol for syngeneic BM chimera mice has been previously described (32). The following BM chimera mice were prepared: male WT BM→female CX3CR1 KO mice, male CX3CR1 KO BM→female WT mice, male WT BM→female WT mice, and male CX3CR1 KO BM→female CX3CR1 KO mice. BM cells were collected from the tibia

Table I. *Sequences of primers used for RT-PCR*

Transcript	Sequence[a]	Product Size (bp)
CXCL1	(F) 5′-GTGTCCCCAAGTAACGGAGA-3′	317
	(R) 5′-TGCACTTCTTTTCGCACAAC-3′	
CXCL2	(F) 5′-GAACAAAGGCAAGGCTAACTGA-3′	204
	(R) 5′-AACATAACAACATCTGGGCAAT-3′	
CXCL9	(F) 5′-AAAATTTCATCACGCCCTTG-3′	207
	(R) 5′-TCTCCAGCTTGGTGAGGTCT-3′	
CXCL10	(F) 5′-GGATGGCTGTCCTAGCTCTG-3′	211
	(R) 5′-ATAACCCCTTGGGAAGATGG-3′	
CCL2	(F) 5′-ACTGAAGCCAGCTCTCTCTTCCTC-3′	274
	(R) 5′-TTCCTTCTTGGGGTCAGCACAGAC-3′	
CCL3	(F) 5′-GCCCTTGCTGTTCTTCTCTGT-3′	258
	(R) 5′-GGCATTCAGTTCCAGGTCAGT-3′	
CCL4	(F) 5′-GCTCTGTGCAAACCTAACCC-3′	360
	(R) 5′-CTGAGGAGGCCTCTCCTGAAGT-3′	
CCL5	(F) 5′-CATATGGCTCGGACACCACT-3′	146
	(R) 5′-ACACACTTGGCGGTTCCTTC-3′	
CX3CL1	(F) 5′-GTTGGCTCCTGAGAGTGAGG-3′	301
	(R) 5′-CAAAATGGCACAGACATTGG-3′	
CXCR2	(F) 5′-ATGCTGTTCTGCTACGGG-3′	282
	(R) 5′-ATGGATGATGGGGTTAAG-3′	
CXCR3	(F) 5′-TGCTAGATGCCTCGGACTTT-3′	214
	(R) 5′-CGCTGACTCAGTAGCACAGC-3′	
CCR1	(F) 5′-GTTGGGACCTTGAACCTTG-3′	250
	(R) 5′-CCCAAAGGCTCTTACAGCAG-3′	
CCR2	(F) 5′-CCTGCAAAGACCAGAAGAGG-3′	382
	(R) 5′-GATGGCCAAGTTGAGCAGAT-3′	
CCR5	(F) 5′-ATTCTCCACACCCTGTTTCG-3′	308
	(R) 5′-CGTTTGACCATGTGTTTTCG-3′	
CX3CR1	(F) 5′-CCTGCCTCTGAGAAATGGAG-3′	332
	(R) 5′-ATCTCTCCAGCCCCTGAAAT-3′	
Collagen type I	(F) 5′-ATCACTGCAAGAACAGCGTA-3′	430
	(R) 5′-TGTTTTCCAAAGTCCATGTG-3′	
TGF-β1	(F) 5′-CGGGGCGACCTGGGCACCATCCATGAC-3′	405
	(R) 5′-CTGCTCCACCTTGGGCTTGCGACCCAC-3′	
VEGF	(F) 5′-TGGATGTCTACCAGCGAAGC-3′	308
	(R) 5′-ACAAGGCTCACAGTGATTTT-3′	
β-actin	(F) 5′-TTCTACAATGAGCTGCGTGTGGC-3′	456
	(R) 5′-CTCATAGCTCTTCTCCAGGGAGGA-3′	

[a] (F), Forward primer; (R), reverse primer.

and femurs of donor mice by aspiration and flushing. Recipient mice received 10 Gy total body irradiation. Then, while under anesthesia, the animals received a suspension of 5×10^6 BM cells i.v. from donor mice in a volume of 200 μl of sterile PBS. For 2 wk after BM transplantation, the mice were housed in sterilized individual cages and were fed normal chow and provided water supplemented with neomycin. To verify successful engraftment, genomic DNA was isolated from peripheral blood and tail tissues of each chimeric mouse 4 and 10 wk after BM transplantation with a NucleoSpin tissue and blood kit (Macherey-Nagel). Then, PCR was performed to detect the *Sry* gene contained in the Y chromosome (forward primer, 5′-TGACACTGGCCTTTTCTCCT-3′; reverse primer, 5′-CATG GCATGCTGTATTGACC-3′). The amplified PCR products were fractionated on a 2% agarose gel and visualized by ethidium bromide staining. After durable BM engraftment was confirmed, mice were generated with skin wounds as described above.

Fluorescence labeling of BM cells with PKH26

Before transplantation, BM cells were labeled ex vivo with PKH26 (Sigma-Aldrich), a red fluorescent dye that emits at 567 nm and has a half-life of >100 days. PKH26 is a lipophilic dye that stains the membrane of viable cells and is distributed between cells when mitosis occurs. Labeling was performed according to the manufacturer's protocol. After labeling, BM cells (5×10^6) were transplanted immediately via tail vein to recipient mice as described above. PKH26-labeled cells were visualized in frozen sections of skin wounds using fluorescence microscopy and appropriate filters.

Statistical analysis

Means and SEs (SEMs) were calculated for all parameters determined in this study. Statistical significance was evaluated by using ANOVA or the Mann-Whitney *U* test. A value of $p < 0.05$ was accepted as statistically significant.

Results

CX3CL1 and CX3CR1 are expressed in wounded skin

We profiled gene expression for 9 inflammatory chemokines (CXCL1, 2, 9, and 10, and CCL2, 3, 4, and 5, and CX3CL1) and 6 inflammatory chemokine receptors (CXCR2 and 3, CCR1, 2, and 5, and CX3CR1) in a mouse model of excisional skin wound healing. All 15 genes were induced in the model to varying extents and with different kinetics (Fig. 1). The results for CXCL1, 2, 9, and 10, CCL2, 3, and 5, CXCR2, and CCR1 confirm and extend previous reports (2, 3, 5–11, 29, 33) and the others are novel. In the present report, we focused on CX3CL1 and CX3CR1, because they were particularly highly induced and not previously characterized.

In WT C57BL/6 mice, CX3CR1 mRNA was weakly detectable in normal unwounded skin (Fig. 1). Wounding induced accumulation of receptor mRNA to high levels by day 3 after injury and this was sustained through the end of the 6-day period of observation. CX3CR1 protein was also expressed in wound sites, specifically on infiltrating F4/80$^+$ macrophages, α-SMA$^+$ fibroblasts, and CD31$^+$ endothelial cells (Fig. 2, *A–C*). Like CX3CR1, CX3CL1 mRNA was also weakly detectable in normal unwounded skin but was increased earlier than the receptor in the

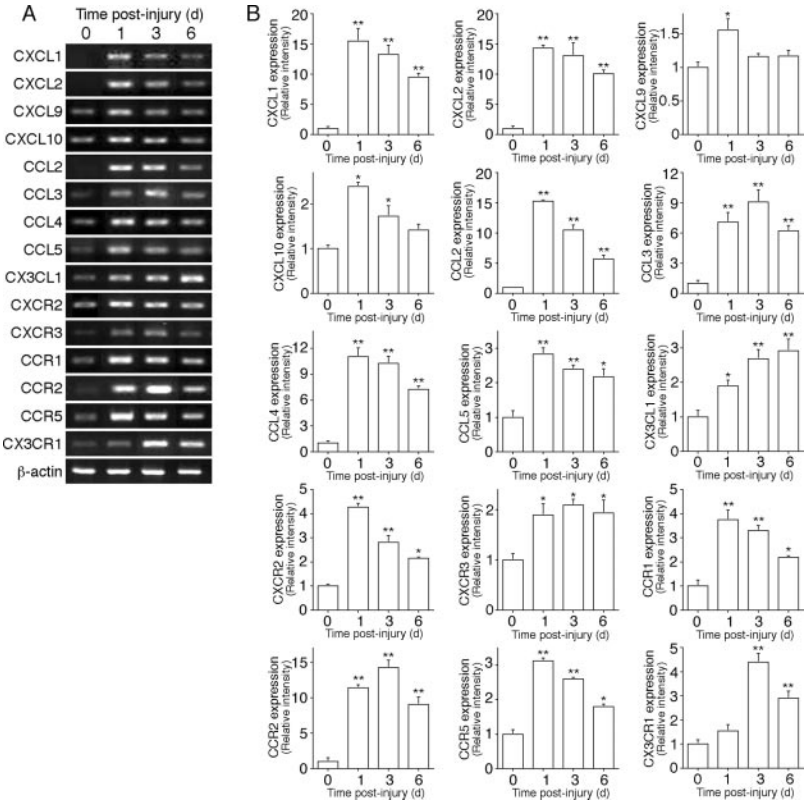

FIGURE 1. Inflammatory chemokines and chemokine receptors are induced in skin of WT C57BL/6 mice by wounding. *A*, RNA analysis. Representative RT-PCR results from three independent experiments with four animals in each group are shown. *B*, Quantitative analysis of data in *A*. The ratios of RT-PCR signals for indicated chemokines and chemokine receptors to β-actin were calculated. Values represent mean ± SEM. **, $p < 0.01$; *, $p < 0.05$, vs uninjured skin (day 0).

wound site (Fig. 1). CX3CL1 mRNA expression increased with linear kinetics throughout the 6-day period of observation after wounding. There were no significant differences in CX3CL1 mRNA expression levels between WT and CX3CR1 KO mice at any time point (data not shown). Immunohistochemical analysis demonstrated CX3CL1 proteins in vascular endothelial cells and infiltrating mononuclear cells in the wound sites (Fig. 3*A*). The infiltrating CX3CL1$^+$ mononuclear cells were identified as mainly F4/80$^+$ macrophages by double immunofluorescence (Fig. 3*B*). Induction of both CX3CR1 and CX3CL1 expression in skin by wounding suggested the hypothesis that functional interaction of this ligand/receptor pair may regulate skin wound healing through an autocrine and/or paracrine mechanism.

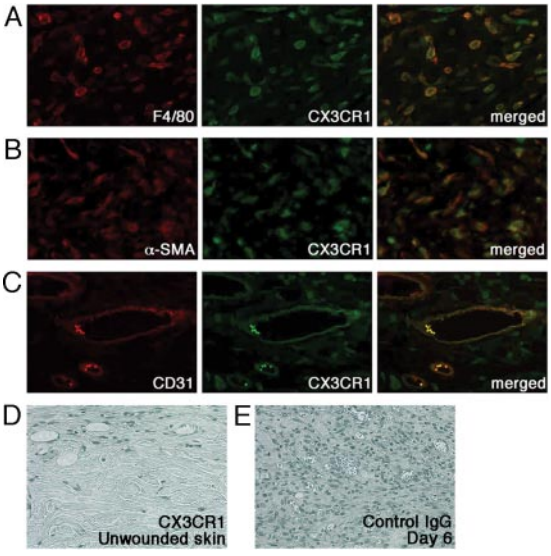

FIGURE 2. CX3CR1 expression is induced at skin wound sites. *A–C*, Cell types expressing CX3CR1 in wounded skin. Double-color immunofluorescence images are shown at day 6 after injury using anti-CX3CR1 (*A–C*), anti-F4/80 (*A*), anti-α-SMA (*B*), and anti-CD31 (*C*), as indicated at the *bottom right* of each panel. Signals were merged digitally in the *right panel* of each row. *D*, Immunohistochemical detection of CX3CR1 on uninjured skin using anti-CX3CR1 Ab. *E*, Control staining of skin wound sites with rabbit IgG 6 days after injury. Representative results from six individual animals are shown. Original magnification, ×320 (*A–C*) and ×200 (*D* and *E*).

CX3CR1 promotes skin wound healing

To test this hypothesis, we first evaluated changes in wound area as a measure of wound closure in WT and CX3CR1 KO mice (Fig. 4). In WT mice, wound areas were reduced with linear kinetics

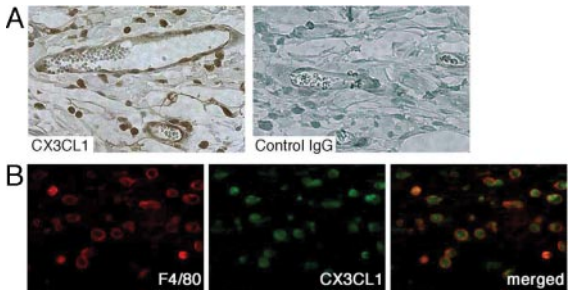

FIGURE 3. CX3CL1 expression is induced at skin wound sites. *A*, Distribution of CX3CL1 protein in skin wound sites. Immunohistochemical analysis was performed using anti-CX3CL1 or control IgG 6 days after injury. Original magnification, ×200. *B*, Determination of cell types expressing CX3CL1 protein in wounded skin. Immunofluorescence was performed with Abs specific for the Ag indicated at the *bottom right* of each panel at day 6 after injury. The fluorescent images were digitally merged in the *right panel*. Original magnification, ×320. Representative results from six individual animals are shown.

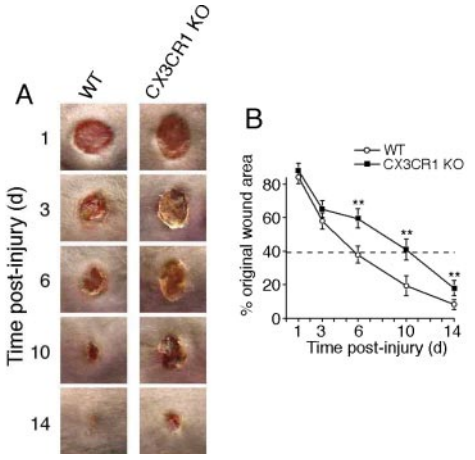

FIGURE 4. CX3CR1 regulates skin wound healing. *A*, Kinetic analysis of skin excisional wound healing. Wound sites were photographed at the time indicated. Representative results from three independent experiments with four animals in each group are shown. *B*, Quantitation of data from *A*. Changes in percentage of wound area at each time point in comparison to the original wound area. Values represent mean ± SEM. **, $p < 0.01$, WT vs CX3CR1 KO mice.

throughout the 14-day period of observation, at the end of which ~95% closure was observed. In contrast, wound closure was significantly delayed in CX3CR1 KO mice (time to 40% wound closure was 6 vs 10 days in WT vs CX3CR1 KO mice, respectively; $p < 0.01$). These observations indicated that germline inactivation of CX3CR1 results in delayed wound healing in C57BL/6 mice.

CX3CR1 regulates accumulation of macrophages, but not neutrophils or T cells, in wounded skin

We next examined the effects of CX3CR1 deficiency on leukocyte infiltration into wounds. Because many neutrophils are trapped within the blood clot that is associated with healing wounds, it is difficult to accurately determine neutrophil number. Thus, we measured MPO activity to evaluate this parameter (Fig. 5). MPO activity reached a peak on day 1, declined thereafter, and was similar in magnitude in WT and CX3CR1 KO mice (Fig. 5*B*). In contrast, F4/80$^+$ macrophages, which were present in small numbers in normal skin, infiltrated the wound sites in large numbers with linear kinetics throughout the 6-day period of observation. Although the kinetics of macrophage infiltration were similar in WT and CX3CR1 KO mice, the magnitudes differed markedly: ~40% lower in CX3CR1 KO mice at day 6 compared with WT mice (Fig. 5, *C* and *D*). Compared with neutrophils and macrophages, CD3$^+$ T cells infiltrated the wound site in small numbers after injury; the kinetics and extent of accumulation were similar in CX3CR1 KO and WT mice (Fig. 5, *E* and *F*). Thus, the absence of CX3CR1 attenuated recruitment of macrophages, but not neutrophils or CD3$^+$ T cells, into the wound sites.

CX3CR1 deficiency does not alter expression of chemokines or other chemokine receptors at skin wound sites

Many CXC and CC chemokines and their receptors were up-regulated after wounding in the model, and typically mRNA expression reached a peak between days 1 and 3 as shown previously in Fig. 1. However, there was no significant difference in expression of any these molecules between WT and CX3CR1 KO mice at any

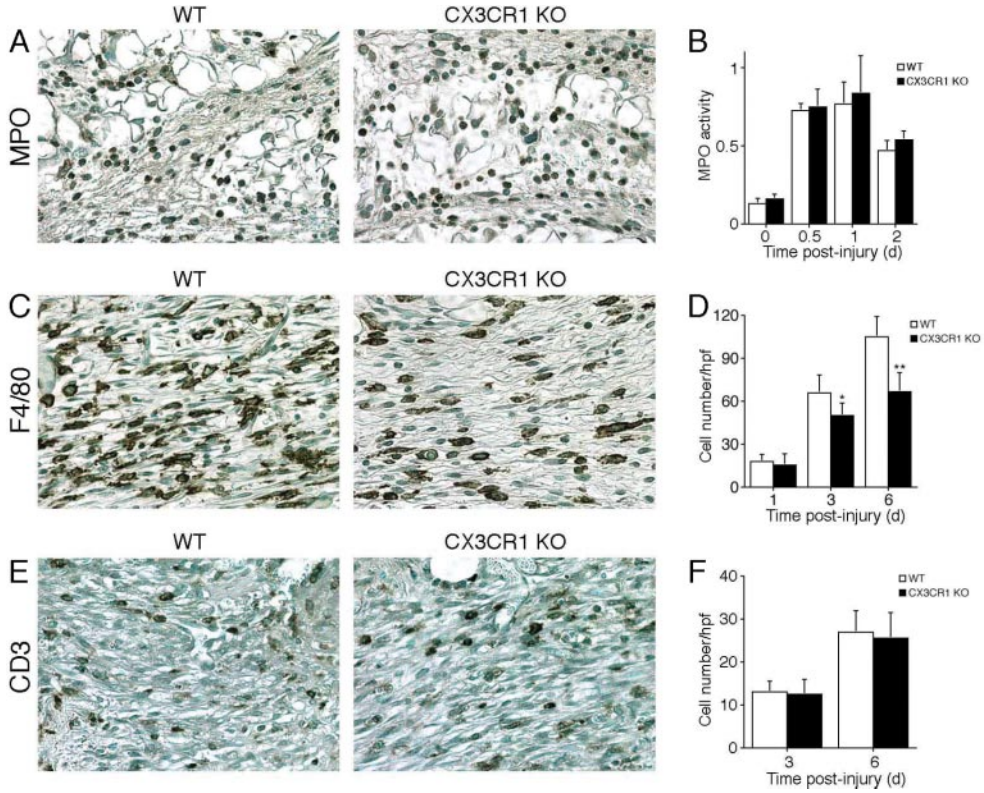

FIGURE 5. CX3CR1 selectively regulates macrophage accumulation at skin wound sites. Immunohistochemical analysis was performed on skin wound samples using anti-MPO (*A*, day 1), anti-F4/80 (*C*, day 6), and anti-CD3 (*E*, day 6) Abs. Representative results from three independent experiments with four animals in each group are shown. Original magnification, ×200. *B*, *D*, and *F*, Quantitation of leukocyte subset accumulation. MPO activity was used to measure neutrophil accumulation (*B*). The numbers of macrophages (*D*) and T cells (*F*) per high-power field were counted (original magnification, ×200). All values represent mean ± SEM. □, WT; ■, CX3CR1 KO mice. **, $p < 0.01$; *, $p < 0.05$, WT vs CX3CR1 KO mice.

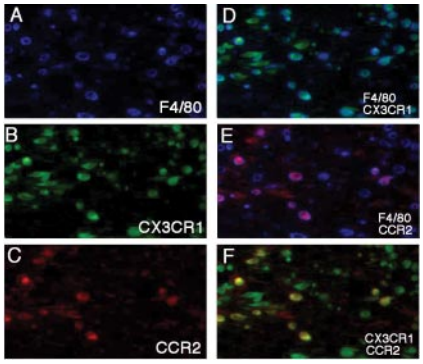

FIGURE 6. $CX3CR1^+CCR2^+$ and $CX3CR1^+CCR2^-$ macrophages accumulate in wounded skin. A triple-color immunofluorescence analysis of wound sites of WT mice was performed using AMCA-labeled anti-F4/80 (*A*), FITC-labeled anti-CX3CR1 (*B*), and Cy3-labeled anti-CCR2 (*C*) Abs at day 6 after injury. The fluorescent images were digitally merged (*D*, F4/80 and CX3CR1; *E*, F4/80 and CCR2; *F*, CX3CR1 and CCR2). Representative results from six individual animals are shown. Original magnification, ×320.

time points (data not shown). These results suggest that CX3CR1 involvement in wound healing may be direct and is not mediated indirectly through effects on expression of other chemokines or chemokine receptors tested.

Both $CX3CR1^+CCR2^-$ and $CX3CR1^+CCR2^+$ macrophage subsets accumulate in wounded skin

Circulating mouse monocytes consist of two functionally distinct subpopulations characterized by the chemokine receptor immunophenotypes $CX3CR1^{high}CCR2^-$ and $CX3CR1^{low}CCR2^+$, which correspond to the $CCR2^-CD16^+$ and $CCR2^+CD16^-$ subsets of human monocytes, respectively (34–38). Therefore, we tested $F4/80^+$ macrophages infiltrating skin wounds for expression of CX3CR1 and CCR2. We detected CX3CR1 protein on most $F4/80^+$ macrophages, consistent with Fig. 2*A* (Fig. 6, *A*, *B*, and *D*), whereas CCR2 was coexpressed on a minority of $F4/80^+$ macrophages (Fig. 6, *A*, *C*, and *E*) at the wound sites 6 days after injury. We found that CX3CR1 expression was more abundant than CCR2 when signals of CX3CR1 and CCR2 were merged (Fig. 6*F*). Therefore, expression of CX3CR1 was more prominent than CCR2 on infiltrating macrophages in skin wounds. These observations suggest that CX3CR1-dependent recruitment of macrophages might be an important mechanism for skin wound healing.

To test this, we analyzed the phenotypes of the following BM chimeric mice (donor BM→recipient) in our model: WT BM→WT, WT BM→CX3CR1 KO, CX3CR1 KO BM→CX3CR1 KO, and CX3CR1 KO BM→WT. BM-derived cells from donor mice were labeled ex vivo with PKH26 red dye, and

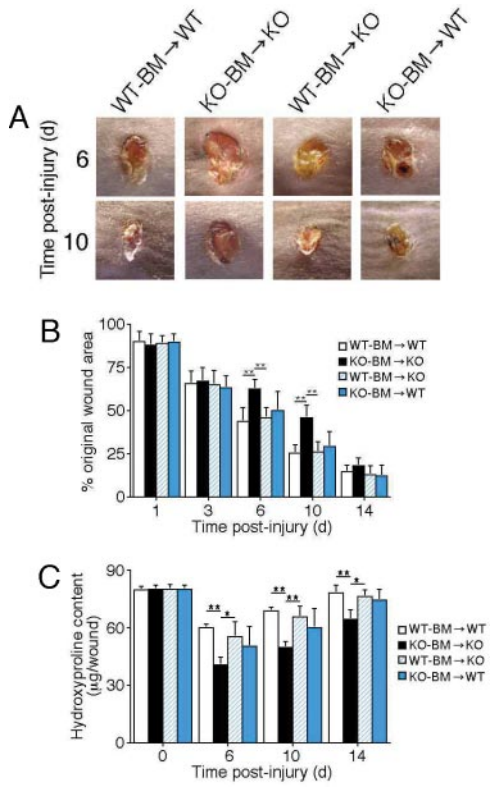

FIGURE 8. Effects of BM transplantation on skin wound healing. Recipient mice were transplanted with BM cells from WT or CX3CR1 KO donors as described in *Materials and Methods*. Excisional wounds were generated in BM chimeric mice 10 wk after BM transplantation. *A*, The wound sites were photographed at days 6 and 10 after injury, and representative results from two independent experiments with at least six animals in each group are shown. *B*, Quantitative analysis of data in *A*. Changes in percentage of wound area at each time point in comparison to the original wound area. *C*, Hydroxyproline content in the wound site. There was no difference in hydroxyproline content among all four BM chimeric mice before injury. All values represent mean ± SEM. ∗, $p < 0.05$; ∗∗, $p < 0.01$, KO-BM→KO vs either WT-BM→WT or WT-BM→KO.

were injected i.v. into lethally irradiated recipients. Skin wounding was performed 10 wk after BM transplantation, and frozen sections of wound sites were prepared and analyzed 6 days later, a time at which macrophages are the predominant BM-derived cell type present in the wound (Fig. 7). Skin sections from transplanted but uninjured control mice contained only a few PKH26-labeled cells in the dermis, whereas wounding caused labeled WT donor BM-derived cells to accumulate in similar large numbers in granulation tissue of both WT and CX3CR1 KO recipients. In contrast,

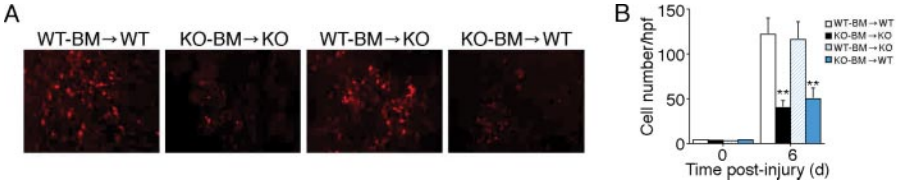

FIGURE 7. BM cells migrate to skin wounds. BM cells from WT and CX3CR1 KO donor mice were labeled with the fluorescent dye PKH26. Labeled cells were injected into the tail vein of irradiated recipient mice as described in *Materials and Methods*. After verifying successful engraftment and reconstitution of the BM in the transplanted mice, excisional wounds were generated. Six days after the injury, wound sites were removed. The migration of PKH26-labeled BM cells to the wound sites was assessed by fluorescent microscopic examination of thin frozen sections. Representative results from six individual animals are shown in *A* (original magnification, ×200). The numbers of PKH26-labeled BM cells per high-power field were counted (*B*). All values represent mean ± SEM. ∗∗, $p < 0.01$, WT-BM→WT vs KO-BM→WT or KO-BM→KO vs WT-BM→KO.

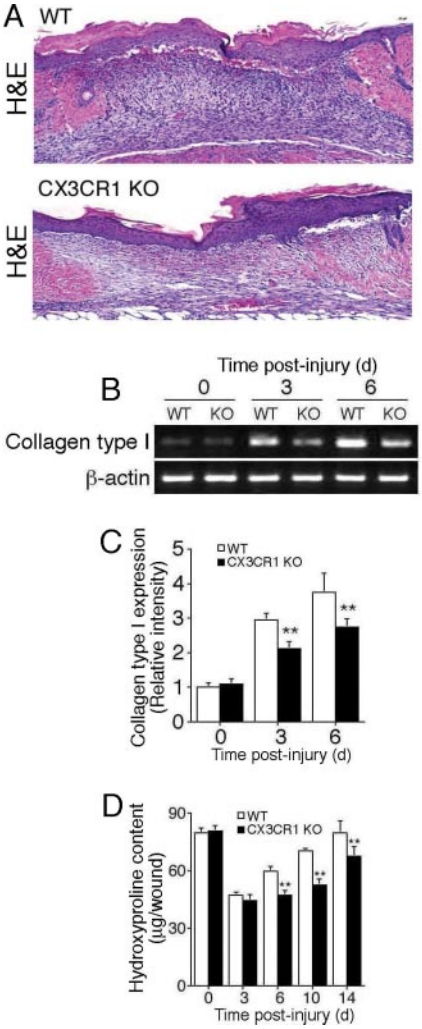

FIGURE 9. CX3CR1 promotes granulation tissue formation and collagen deposition in wounded skin. *A*, Granulation tissue. Histopathological analysis was performed at day 6 after injury. Representative results from six individual animals are shown in *A* (H&E; magnification ×50). *B–D*, Collagen deposition. RT-PCR analysis of collagen type I gene expression at the wound sites. Representative results from three independent experiments with four animals in each group are shown in *B*. The ratios of collagen type I to β-actin are shown in *C*. *D*, Hydroxyproline content in wound sites. All values represent mean ± SEM. **, $p < 0.01$, WT vs CX3CR1 KO mice.

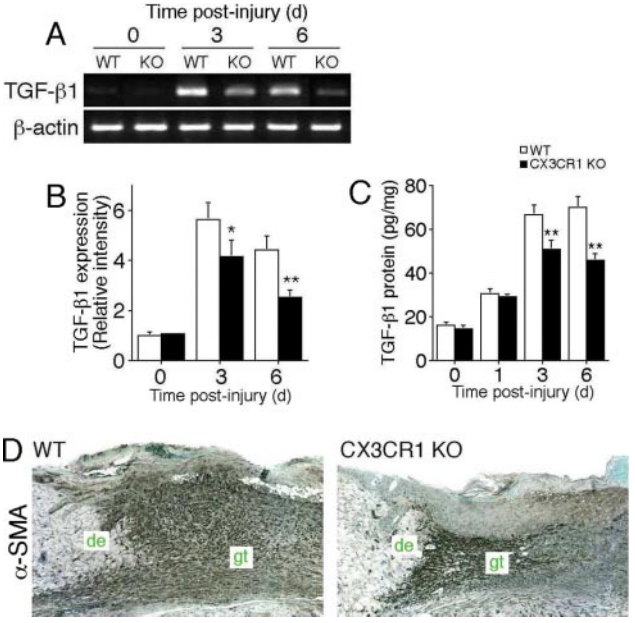

FIGURE 10. CX3CR1 promotes TGF-β1 expression and activated fibroblast accumulation in wounded skin. *A* and *B*, RT-PCR analysis of TGF-β1 gene expression in the wound sites. Representative results from three independent experiments with four animals in each group are shown in *A*. The ratios of TGF-β1 to β-actin are shown in *B*. *C*, TGF-β1 protein contents in skin wounds by ELISA. Values represent mean ± SEM. **, $p < 0.01$; *, $p < 0.05$, WT vs CX3CR1 KO mice. *D*, Immunohistochemical analysis of α-SMA, a key marker for myofibroblast differentiation and wound contraction, on wound tissue sections at day 6 after injury. Representative results from six individual animals are shown in *D*. Original magnification, ×80; de, adjacent dermis; gt, granulation tissue.

accumulation of labeled cells at the wound site was markedly reduced to a similar extent (~60%) in both CX3CR1 KO and WT recipient mice when CX3CR1 KO donor BM was transferred. Thus, CX3CR1 expression mediated accumulation of most, but not all, donor BM-derived cells at wound sites 6 days after wounding, suggesting a direct functional role for the receptor on macrophage accumulation in the wound.

Because CX3CR1 in the wound site is located on both macrophages, which originate in BM, and fibroblasts, we next attempted to distinguish the role in repair of receptor expression on each of these cell types. To do so, we analyzed wound closure and collagen deposition in BM-chimeric mice. As expected, both wound closure and hydroxyproline accumulation were significantly delayed over the 14-day period of observation in CX3CR1 KO recipient mice transplanted with CX3CR1 KO donor BM, as compared with the positive control (WT recipients of WT donor BM cells). However, hydroxyproline and wound healing kinetics were also equivalent to the positive control when either the donor BM or the recipient mouse, but not both, were CX3CR1 KO (Fig. 8). Thus, defective wound healing results when CX3CR1 is missing from both a BM-derived cell, probably a macrophage, and a non-BM-derived cell, possibly a fibroblast.

CX3CR1 promotes granulation tissue formation and collagen deposition in wounded skin

We next directly examined the role of CX3CR1 on collagen accumulation in wounded mice by histopathology. Granulation tissue formation was markedly reduced at the wound sites in CX3CR1 KO mice compared with WT mice at day 6 (Fig. 9*A*). In uninjured skin (time = 0), there was no significant difference in collagen type I mRNA expression (Fig. 9, *B* and *C*) or hydroxyproline content (Fig. 9*D*) between CX3CR1 KO mice and WT mice. Compared with this baseline, skin wounding induced collagen type I mRNA expression in WT mice throughout the 6-day time course of observation after injury, whereas induction was significantly reduced in CX3CR1 KO mice (Fig. 9, *B* and *C*). Accordingly, the normal increase in hydroxyproline content at wound sites was significantly decreased in CX3CR1 KO mice throughout the 14-day time course of observation (Fig. 9*D*). Thus, CX3CR1 deficiency caused a reduction in collagen deposition and eventually delayed granulation tissue formation in the model.

CX3CR1 promotes TGF-β1 expression and myofibroblast accumulation in wounded skin

Because TGF-β1 has been shown to control key steps in granulation tissue formation, such as fibroblast influx, myofibroblast induction, formation of extracellular matrix, and cell proliferation (2,

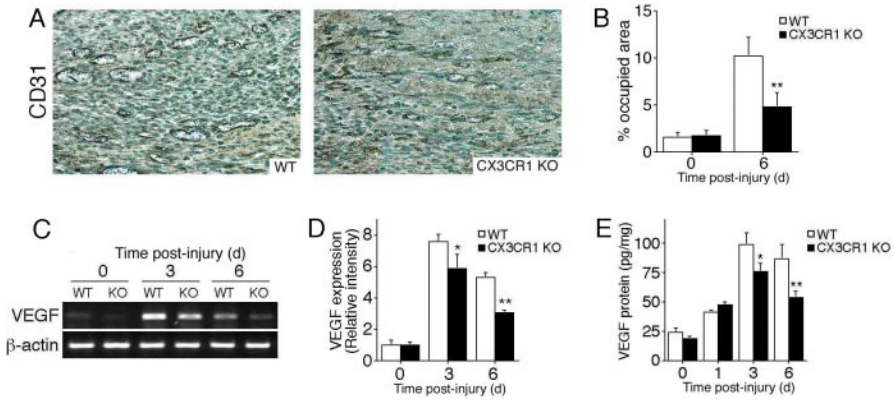

FIGURE 11. CX3CR1 promotes neovascularization and VEGF expression in wounded skin. *A*, Neovascularization. Immunohistochemical analysis with anti-CD31 mAb 6 days after injury. Representative results from six individual animals are shown. Original magnification, ×200. *B*, Quantitation of data in *A*. The vascular areas were identified as CD31-positive areas with Adobe PhotoShop. *C* and *D*, VEGF gene expression. Representative results of RT-PCR analysis are shown in *C*. The ratios of VEGF to β-actin signal are shown in *D*. *E*, VEGF protein content in skin wounds by ELISA. All values represent mean ± SEM from three independent experiments with four animals in each time point. **, $p < 0.01$; *, $p < 0.05$, WT vs CX3CR1 KO mice.

39–41), we examined TGF-β1 levels at wound sites as a function of CX3CR1. Normal wound-induced enhancement of TGF-β1 gene expression was significantly attenuated in CX3CR1 KO mice compared with WT mice at days 3 and 6 after injury (Fig. 10, *A* and *B*). This result was confirmed at the protein level in wound tissue lysates using an ELISA specific for active TGF-β1 (Fig. 10*C*). Consistent with this, immunohistochemical analysis with the myofibroblast marker α-SMA 6 days after injury demonstrated that myofibroblasts were abundant at the wound edges of WT mice, but relatively deficient in the same location of wounds from CX3CR1 KO mice (Fig. 10*D*). These results suggest that CX3CR1 activity in vivo promotes TGF-β1 production, which promotes accumulation of α-SMA$^+$-activated fibroblasts, which are the direct source of collagen, a key constituent of granulation tissue in skin wound repair.

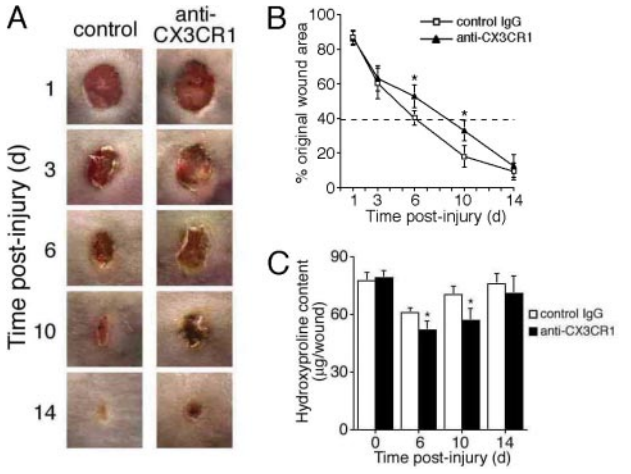

FIGURE 12. CX3CR1 neutralization suppresses excisional skin wound closure and hydroxyproline accumulation. *A* and *B*, Wound closure. The wound sites were photographed at the times indicated in *A*. Representative results from three independent experiments with four animals in each group are shown in *A*. *B*, Changes in percentage of wound area at each time point in comparison to the original wound area. *C*, Hydroxyproline content. □, WT treated with control IgG; ■, WT treated with anti-CX3CR1 Abs. All values represent mean ± SEM. *, $p < 0.05$, control IgG vs anti-CX3CR1.

CX3CR1 promotes VEGF production and angiogenesis in wounded skin

Angiogenesis, the growth and proliferation of new blood vessels, is another important aspect of the wound healing process, thus we next examined the effect of CX3CR1 deficiency on neovascularization at wound sites. Using immunohistochemical analysis with anti-CD31, no significant difference was observed in the vessel density of uninjured skin (time = 0) between WT and CX3CR1 KO mice (Fig. 11, *A* and *B*). Six days after injury, the vessel density within the wound bed was increased in both WT and CX3CR1 KO mice, but was significantly decreased in CX3CR1 KO mice compared with WT mice (Fig. 11, *A* and *B*). Consistent with this, VEGF mRNA (Fig. 11, *C* and *D*) and protein expression (Fig. 11*E*) in the wound sites was significantly decreased in CX3CR1 KO mice compared with WT mice throughout the time course of observation. These data imply that the absence of CX3CR1 may interfere with angiogenesis in skin wound sites, at least partly by reducing VEGF expression.

Neutralizing anti-CX3CR1 Abs impair skin wound healing

To clarify the role of CX3CR1 during skin wound healing directly, WT mice were injected with neutralizing anti-CX3CR1 Abs or control IgG. The administration of neutralizing anti-CX3CR1 Abs retarded the wound closure rate in WT mice compared with controls (time to 40% wound closure was 6 vs 9 days in control IgG- vs anti-CX3CR1-injected WT mice, respectively) (Fig. 12, *A* and *B*). Moreover, CX3CR1 neutralization significantly diminished hydroxyproline content in the wound sites at days 6 and 10 after injury (Fig. 12*C*). These observations indicate that as with *CX3CR1* gene disruption, CX3CR1 neutralization impairs collagen deposition, wound closure, and subsequent wound healing.

Discussion

In the present study, we have demonstrated genetically and by immunologic blockade that the chemokine receptor CX3CR1 regulates skin wound healing in a mouse model. Multiple reparative processes were affected by the receptor, including inflammation, fibrosis, neovascularization, and regeneration of parenchymal cells. The results are consistent with previous reports showing that the CX3CL1-CX3CR1 ligand-receptor pair plays an important role in the initiation and progression of inflammation (12–14), and is

up-regulated in inflammatory diseases (20–23, 26, 27, 42), including inflammatory diseases of the skin (15, 16, 19). Our data linking CX3CR1 to fibrosis in skin wound healing are consistent with a report of CX3CL1 and CX3CR1 expression in the skin and lung of patients with systemic sclerosis (16), and an in vivo study showing that CX3CR1 KO mice have reduced collagen accumulation and renal fibrosis in a model of ischemia-reperfusion injury (18).

CX3CL1 is the only known ligand for CX3CR1. Expressed as a transmembrane protein on the plasma membrane, CX3CL1 may be subsequently cleaved by proteases such as ADAM10, resulting in a soluble or shed agonist. The membrane form mediates cell-cell adhesion whereas the shed form mediates chemotactic and anti-apoptotic responses. This complicates considerations of how CX3CR1 functions at the cellular level in biological contexts. Moreover, consistent with previous reports in other biological contexts (16, 18, 21–23, 43, 44), in wounded skin both CX3CL1 and CX3CR1 were detectable on macrophages and endothelial cells, and CX3CR1 was detectable on fibroblasts. In this regard, membrane-bound CX3CL1-CX3CR1 interactions could in principle directly mediate homotypic adhesion of macrophages, and/or directly mediate heterotypic adhesion between macrophage and fibroblast, macrophage and endothelial cell, and/or fibroblast and endothelial cell. In addition, shed CX3CL1 could in principle directly recruit/activate macrophages, fibroblasts, and endothelial cells, by acting at CX3CR1. In addition, there is the potential for indirect autocrine and paracrine effects initiated by CX3CR1-dependent activation of macrophages, fibroblasts, and/or endothelial cells.

Among these possibilities, our data provide strong evidence in vivo that CX3CR1 directly mediates macrophage accumulation at the wound site. First, both ligand and receptor were induced at wound sites by wounding, with CX3CL1 induction occurring on cells resident in the skin and CX3CR1 occurring on infiltrating macrophages; moreover, CX3CL1 induction slightly preceded CX3CR1. Second, CX3CR1 was expressed on virtually all macrophages at the wound site. Third, CX3CR1 deficiency markedly reduced macrophage accumulation in wounded skin. Fourth, mRNA levels of various other inflammatory chemokines and chemokine receptors were up-regulated after skin wounding, but were unaffected in CX3CR1-deficient mice. Fifth, labeled BM-derived cells from WT donor mice accumulated in large numbers in wound sites of both recipient WT and CX3CR1 KO mice on day 6 after injury, a time point when macrophages are the major leukocyte subset found in the wound, whereas accumulation was markedly reduced when the donor mouse was CX3CR1 KO. A similar role for CX3CR1 in mediating macrophage accumulation in diseased tissue has been reported in a mouse model of atherosclerosis, and CX3CR1 has been implicated directly in human atherosclerotic cardiovascular disease (26, 45, 46). However, heretofore the chemokine signals regulating macrophage accumulation in healing wounds had not been clearly delineated.

Our study opens up many new questions. The reconstituting BM-derived cell type(s) may be further defined by approaches such as transfer of sorted and labeled BM-derived cells or gene targeting of CX3CR1 in specific lineages. How CX3CR1 works in the model requires further definition: does it only promote monocyte/macrophage influx from the blood into the wound as the transfer experiments suggest, or does it also mediate macrophage retention in the wound? CX3CL1-CX3CR1 signaling has also been reported to maintain cell survival and inhibit Fas-dependent cell death of brain microglia in vitro (47). Perhaps it also regulates survival of dermal macrophages in wounded skin. The reconstitution experiments suggest that BM, which contains inflammatory cell progenitors, mesenchymal stem cells, and multipotent stem cells (48–50), could be used to promote healing of chronic wounds.

It is important to note that CX3CR1 deficiency did not completely abrogate macrophage accumulation in wounded skin, and that macrophages express other chemoattractant receptors which could act in a coordinated, sequential manner to achieve complete monocyte/macrophage recruitment into the wounds (3, 8, 51). This caveat is particularly important because the adoptive transfer experiments clearly showed that CX3CR1 deficiency is required on both BM-derived cells and non-BM-derived cells to delay wound healing in the model. A good candidate is the important macrophage chemoattractant CCL2. This chemokine acts through the receptor CCR2, which is expressed on a subset of $CX3CR1^+$ macrophages in wounded skin. Moreover, it is able to induce CX3CR1 expression on monocytes (52). CCL2 is produced earlier than CX3CL1 in the model and, in functional tests, immunoneutralization of CCL2 reduced macrophage migration into wounded mouse skin (9). However, genetic disruption of CCL2 did not (7), possibly due to development of a compensatory mechanism when CCL2 function is abolished in the germline. In addition to recruiting monocytes from the blood to the wound site, CCR2 might also be required for monocytes to emigrate from the bone marrow to the peripheral circulation, as has been shown in a mouse model of listeriosis (53).

The relevant $CX3CR1^+$ non-BM-derived cell type(s) important in wound healing most likely include resident cells such as dermal fibroblasts and endothelial cells, which we showed were both $CX3CR1^+$ directly in wounded skin. CX3CL1-CX3CR1 interaction may contribute directly to the accumulation and function of these cell types within wounds. However, our data also implicate indirect paracrine mechanisms involving wound macrophages, which have been shown to initiate the proliferative phase of wound healing by releasing a number of growth factors, including VEGF and TGF-β, which are potent inducers of angiogenesis and fibrosis (2, 54, 55). Consistent with this, both TGF-β1 expression and collagen deposition were decreased at wound sites in CX3CR1 KO mice in association with decreased macrophage accumulation. After migration, fibroblasts may differentiate in a TGF-β1-dependent manner into myofibroblasts, which are specialized cells with high synthetic capacity for extracellular matrix components, including collagen, thereby causing fibrotic changes (39–41, 56, 57). Consistent with this, α-SMA^+ myofibroblasts and granulation tissue were diminished at the wound sites in CX3CR1 KO mice.

During wound healing, chemokines exert their regulatory activity on angiogenesis directly or as a consequence of leukocyte infiltration and the induction of growth factor expression (7, 10, 11, 58, 59). Recent studies have implicated CX3CL1 directly in endothelial cell migration and tube formation in vitro and angiogenesis in vivo (43, 44). These observations imply that the CX3CL1-CX3CR1 system may function as an angiogenic mediator in skin wound healing. Consistent with this, our data showed directly by immunohistochemistry that neovascularization was markedly diminished at wound sites of CX3CR1 KO mice. Also, although CX3CL1 directly stimulates angiogenesis, the local microvasculature also depends on several other growth factors, including VEGF and TGF-β, which are produced by macrophages in wounds (60–64). TGF-β signaling is able to up-regulate VEGF expression in various cell types (65–68). We also found significant decreases in VEGF gene expression at wound sites in CX3CR1 KO mice. Thus, CX3CL1-CX3CR1 signaling may stimulate angiogenesis directly and/or indirectly during wound healing.

In summary, we have shown that CX3CR1 is important in wound healing in a mouse model. The mechanism includes effects

on both CX3CR1$^+$ BM-derived cells, most likely monocytes/macrophages, and CX3CR1$^+$ non-BM-derived cells, most likely fibroblasts and endothelial cells. We show that CX3CR1 is important for macrophage accumulation in the wound site and that angiogenic and profibrotic macrophage products are reduced in wounded skin in the absence of CX3CR1. This is associated with impaired myofibroblast accumulation, collagen deposition, fibrosis, angiogenesis, and granulation tissue formation. The results suggest that stimulating CX3CR1 in wounds may accelerate healing, and could be beneficial in the context of surgery, chronic ulcers, and other pathologic conditions.

Acknowledgment

We thank Dr. Toshikazu Kondo (Wakayama Medical University, Japan) for technical advice.

Disclosures

The authors have no financial conflict of interest.

References

1. Singer, A. J., and R. A. Clark. 1999. Cutaneous wound healing. *N. Engl. J. Med.* 341: 738–746.
2. Werner, S., and R. Grose. 2003. Regulation of wound healing by growth factors and cytokines. *Physiol. Rev.* 83: 835–870.
3. Gillitzer, R., and M. Goebeler. 2001. Chemokines in cutaneous wound healing. *J. Leukocyte Biol.* 69: 513–521.
4. Martin, P., and S. J. Leibovich. 2005. Inflammatory cells during wound repair: the good, the bad and the ugly. *Trends Cell. Biol.* 15: 599–607.
5. Mori, R., T. Kondo, T. Ohshima, Y. Ishida, and N. Mukaida. 2002. Accelerated wound healing in tumor necrosis factor receptor p55-deficient mice with reduced leukocyte infiltration. *FASEB J.* 16: 963–974.
6. Lin, Z. Q., T. Kondo, Y. Ishida, T. Takayasu, and N. Mukaida. 2003. Essential involvement of IL-6 in the skin wound-healing process as evidenced by delayed wound healing in IL-6-deficient mice. *J. Leukocyte Biol.* 73: 713–721.
7. Low, Q. E., I. A. Drugea, L. A. Duffner, D. G. Quinn, D. N. Cook, B. J. Rollins, E. J. Kovacs, and L. A. DiPietro. 2001. Wound healing in MIP-1$\alpha^{-/-}$ and MCP-1$^{-/-}$ mice. *Am. J. Pathol.* 159: 457–463.
8. Engelhardt, E., A. Toksoy, M. Goebeler, S. Debus, E. B. Brocker, and R. Gillitzer. 1998. Chemokines IL-8, GROα, MCP-1, IP-10, and Mig are sequentially and differentially expressed during phase-specific infiltration of leukocyte subsets in human wound healing. *Am. J. Pathol.* 153: 1849–1860.
9. Dipietro, L. A., M. G. Reintjes, Q. E. Low, B. Levi, and R. L. Gamelli. 2001. Modulation of macrophage recruitment into wounds by monocyte chemoattractant protein-1. *Wound Repair Regen.* 9: 28–33.
10. Devalaraja, R. M., L. B. Nanney, J. Du, Q. Qian, Y. Yu, M. N. Devalaraja, and A. Richmond. 2000. Delayed wound healing in CXCR2 knockout mice. *J. Invest. Dermatol.* 115: 234–244.
11. Luster, A. D., R. D. Cardiff, J. A. MacLean, K. Crowe, and R. D. Granstein. 1998. Delayed wound healing and disorganized neovascularization in transgenic mice expressing the IP-10 chemokine. *Proc. Assoc. Am. Physicians* 110: 183–196.
12. Bazan, J. F., K. B. Bacon, G. Hardiman, W. Wang, K. Soo, D. Rossi, D. R. Greaves, A. Zlotnik, and T. J. Schall. 1997. A new class of membrane-bound chemokine with a CX_3C motif. *Nature* 385: 640–644.
13. Fong, A. M., L. A. Robinson, D. A. Steeber, T. F. Tedder, O. Yoshie, T. Imai, and D. D. Patel. 1998. Fractalkine and CX_3CR1 mediate a novel mechanism of leukocyte capture, firm adhesion, and activation under physiologic flow. *J. Exp. Med.* 188: 1413–1419.
14. Imai, T., K. Hieshima, C. Haskell, M. Baba, M. Nagira, M. Nishimura, M. Kakizaki, S. Takagi, H. Nomiyama, T. J. Schall, and O. Yoshie. 1997. Identification and molecular characterization of fractalkine receptor CX_3CR1, which mediates both leukocyte migration and adhesion. *Cell* 91: 521–530.
15. Echigo, T., M. Hasegawa, Y. Shimada, K. Takehara, and S. Sato. 2004. Expression of fractalkine and its receptor, CX_3CR1, in atopic dermatitis: possible contribution to skin inflammation. *J. Allergy Clin. Immunol.* 113: 940–948.
16. Hasegawa, M., S. Sato, T. Echigo, Y. Hamaguchi, M. Yasui, and K. Takehara. 2005. Up regulated expression of fractalkine/CX_3CL1 and CX_3CR1 in patients with systemic sclerosis. *Ann. Rheum. Dis.* 64: 21–28.
17. Harrison, J. K., Y. Jiang, S. Chen, Y. Xia, D. Maciejewski, R. K. McNamara, W. J. Streit, M. N. Salafranca, S. Adhikari, D. A. Thompson, et al. 1998. Role for neuronally derived fractalkine in mediating interactions between neurons and CX3CR1-expressing microglia. *Proc. Natl. Acad. Sci. USA* 95: 10896–10901.
18. Furuichi, K., J. L. Gao, and P. M. Murphy. 2006. Chemokine receptor CX3CR1 regulates renal interstitial fibrosis after ischemia-reperfusion injury. *Am. J. Pathol.* 169: 372–387.
19. Raychaudhuri, S. P., W. Y. Jiang, and E. M. Farber. 2001. Cellular localization of fractalkine at sites of inflammation: antigen-presenting cells in psoriasis express high levels of fractalkine. *Br. J. Dermatol.* 144: 1105–1113.
20. Muehlhoefer, A., L. J. Saubermann, X. Gu, K. Luedtke-Heckenkamp, R. Xavier, R. S. Blumberg, D. K. Podolsky, R. P. MacDermott, and H. C. Reinecker. 2000. Fractalkine is an epithelial and endothelial cell-derived chemoattractant for intraepithelial lymphocytes in the small intestinal mucosa. *J. Immunol.* 164: 3368–3376.
21. Ruth, J. H., M. V. Volin, G. K. Haines, 3rd, D. C. Woodruff, K. J. Katschke, Jr., J. M. Woods, C. C. Park, J. C. Morel, and A. E. Koch. 2001. Fractalkine, a novel chemokine in rheumatoid arthritis and in rat adjuvant-induced arthritis. *Arthritis Rheum.* 44: 1568–1581.
22. Lucas, A. D., C. Bursill, T. J. Guzik, J. Sadowski, K. M. Channon, and D. R. Greaves. 2003. Smooth muscle cells in human atherosclerotic plaques express the fractalkine receptor CX_3CR1 and undergo chemotaxis to the CX_3C chemokine fractalkine (CX_3CL1). *Circulation* 108: 2498–2504.
23. Feng, L., S. Chen, G. E. Garcia, Y. Xia, M. A. Siani, P. Botti, C. B. Wilson, J. K. Harrison, and K. B. Bacon. 1999. Prevention of crescentic glomerulonephritis by immunoneutralization of the fractalkine receptor CX_3CR1 rapid communication. *Kidney Int.* 56: 612–620.
24. Lapidot, T., and I. Petit. 2002. Current understanding of stem cell mobilization: the roles of chemokines, proteolytic enzymes, adhesion molecules, cytokines, and stromal cells. *Exp. Hematol.* 30: 973–981.
25. Kucia, M., W. Wojakowski, R. Reca, B. Machalinski, J. Gozdzik, M. Majka, J. Baran, J. Ratajczak, and M. Z. Ratajczak. 2006. The migration of bone marrow-derived non-hematopoietic tissue-committed stem cells is regulated in an SDF-1-, HGF-, and LIF-dependent manner. *Arch. Immunol. Ther. Exp.* 54: 121–135.
26. Combadiere, C., S. Potteaux, J. L. Gao, B. Esposito, S. Casanova, E. J. Lee, P. Debre, A. Tedgui, P. M. Murphy, and Z. Mallat. 2003. Decreased atherosclerotic lesion formation in CX3CR1/apolipoprotein E double knockout mice. *Circulation* 107: 1009–1016.
27. Robinson, L. A., C. Nataraj, D. W. Thomas, D. N. Howell, R. Griffiths, V. Bautch, D. D. Patel, L. Feng, and T. M. Coffman. 2000. A role for fractalkine and its receptor (CX_3CR1) in cardiac allograft rejection. *J. Immunol.* 165: 6067–6072.
28. Donadelli, R., C. Zanchi, M. Morigi, S. Buelli, C. Batani, S. Tomasoni, D. Corna, D. Rottoli, A. Benigni, M. Abbate, et al. 2003. Protein overload induces fractalkine upregulation in proximal tubular cells through nuclear factor κB- and p38 mitogen-activated protein kinase-dependent pathways. *J. Am. Soc. Nephrol.* 14: 2436–2446.
29. Ishida, Y., T. Kondo, A. Kimura, K. Matsushima, and N. Mukaida. 2006. Absence of IL-1 receptor antagonist impaired wound healing along with aberrant NF-κB activation and a reciprocal suppression of TGF-β signal pathway. *J. Immunol.* 176: 5598–5606.
30. Ishida, Y., T. Kondo, T. Takayasu, Y. Iwakura, and N. Mukaida. 2004. The essential involvement of cross-talk between IFN-γ and TGF-β in the skin wound-healing process. *J. Immunol.* 172: 1848–1855.
31. Ishida, Y., T. Maegawa, T. Kondo, A. Kimura, Y. Iwakura, S. Nakamura, and N. Mukaida. 2004. Essential involvement of IFN-γ in *Clostridium difficile* toxin A-induced enteritis. *J. Immunol.* 172: 3018–3025.
32. Ishida, Y., A. Kimura, T. Kondo, T. Hayashi, M. Ueno, N. Takakura, K. Matsushima, and N. Mukaida. 2007. Essential roles of the CC chemokine ligand 3-CC chemokine receptor 5 axis in bleomycin-induced pulmonary fibrosis through regulation of macrophage and fibrocyte infiltration. *Am. J. Pathol.* 170: 843–854.
33. Kaesler, S., P. Bugnon, J. L. Gao, P. M. Murphy, A. Goppelt, and S. Werner. 2004. The chemokine receptor CCR1 is strongly up-regulated after skin injury but dispensable for wound healing. *Wound Repair Regen.* 12: 193–204.
34. Ancuta, P., R. Rao, A. Moses, A. Mehle, S. K. Shaw, F. W. Luscinskas, and D. Gabuzda. 2003. Fractalkine preferentially mediates arrest and migration of CD16$^+$ monocytes. *J. Exp. Med.* 197: 1701–1707.
35. Geissmann, F., S. Jung, and D. R. Littman. 2003. Blood monocytes consist of two principal subsets with distinct migratory properties. *Immunity* 19: 71–82.
36. Robben, P. M., M. LaRegina, W. A. Kuziel, and L. D. Sibley. 2005. Recruitment of Gr-1$^+$ monocytes is essential for control of acute toxoplasmosis. *J. Exp. Med.* 201: 1761–1769.
37. Gordon, S., and P. R. Taylor. 2005. Monocyte and macrophage heterogeneity. *Nat. Rev. Immunol.* 5: 953–964.
38. Grage-Griebenow, E., H. D. Flad, and M. Ernst. 2001. Heterogeneity of human peripheral blood monocyte subsets. *J. Leukocyte Biol.* 69: 11–20.
39. Border, W. A., and N. A. Noble. 1994. Transforming growth factor β in tissue fibrosis. *N. Engl. J. Med.* 331: 1286–1292.
40. Kovacs, E. J., and L. A. DiPietro. 1994. Fibrogenic cytokines and connective tissue production. *FASEB J.* 8: 854–861.
41. Gabbiani, G. 2003. The myofibroblast in wound healing and fibrocontractive diseases. *J. Pathol.* 200: 500–503.
42. Tong, N., S. W. Perry, Q. Zhang, H. J. James, H. Guo, A. Brooks, H. Bal, S. A. Kinnear, S. Fine, L. G. Epstein, et al. 2000. Neuronal fractalkine expression in HIV-1 encephalitis: roles for macrophage recruitment and neuroprotection in the central nervous system. *J. Immunol.* 164: 1333–1339.
43. Volin, M. V., J. M. Woods, M. A. Amin, M. A. Connors, L. A. Harlow, and A. E. Koch. 2001. Fractalkine: a novel angiogenic chemokine in rheumatoid arthritis. *Am. J. Pathol.* 159: 1521–1530.
44. Lee, S. J., S. Namkoong, Y. M. Kim, C. K. Kim, H. Lee, K. S. Ha, H. T. Chung, Y. G. Kwon, and Y. M. Kim. 2006. Fractalkine stimulates angiogenesis by activating the Raf-1/MEK/ERK- and PI3K/Akt/eNOS-dependent signal pathways. *Am. J. Physiol.* 291: H2836–H2846.
45. Barlic, J., Y. Zhang, and P. M. Murphy. 2007. Atherogenic lipids induce adhesion of human coronary artery smooth muscle cells to macrophages by up-regulating chemokine CX3CL1 on smooth muscle cells in a TNFα-NFκB-dependent manner. *J. Biol. Chem.* 282: 19167–19176.

46. Lesnik, P., C. A. Haskell, and I. F. Charo. 2003. Decreased atherosclerosis in $CX_3CR1^{-/-}$ mice reveals a role for fractalkine in atherogenesis. *J. Clin. Invest.* 111: 333–340.
47. Boehme, S. A., F. M. Lio, D. Maciejewski-Lenoir, K. B. Bacon, and P. J. Conlon. 2000. The chemokine fractalkine inhibits Fas-mediated cell death of brain microglia. *J. Immunol.* 165: 397–403.
48. Badiavas, E. V., and V. Falanga. 2003. Treatment of chronic wounds with bone marrow-derived cells. *Arch. Dermatol.* 139: 510–516.
49. Badiavas, E. V. 2004. The potential of bone marrow cells to orchestrate homeostasis and healing in skin. *Blood Cells Mol. Dis.* 32: 21–23.
50. Cha, J., and V. Falanga. 2007. Stem cells in cutaneous wound healing. *Clin. Dermatol.* 25: 73–78.
51. Jackman, S. H., M. B. Yoak, S. Keerthy, and B. L. Beaver. 2000. Differential expression of chemokines in a mouse model of wound healing. *Ann. Clin. Lab. Sci.* 30: 201–207.
52. Green, S. R., K. H. Han, Y. Chen, F. Almazan, I. F. Charo, Y. I. Miller, and O. Quehenberger. 2006. The CC chemokine MCP-1 stimulates surface expression of CX3CR1 and enhances the adhesion of monocytes to fractalkine/CX3CL1 via p38 MAPK. *J. Immunol.* 176: 7412–7420.
53. Serbina, N. V., and E. G. Pamer. 2006. Monocyte emigration from bone marrow during bacterial infection requires signals mediated by chemokine receptor CCR2. *Nat. Immunol.* 7: 311–317.
54. DiPietro, L. A. 1995. Wound healing: the role of the macrophage and other immune cells. *Shock* 4: 233–240.
55. Riches, D. 1996. Macrophage involvement in wound repair, remodeling, and fibrosis. In *The Molecular and Cellular Biology of Wound Repair*, 2nd Ed. R. A. F. Clark, ed. Plenum Press, New York, pp. 95–141.
56. Midwood, K. S., L. V. Williams, and J. E. Schwarzbauer. 2004. Tissue repair and the dynamics of the extracellular matrix. *Int. J. Biochem. Cell. Biol.* 36: 1031–1037.
57. Hu, B., Z. Wu, and S. H. Phan. 2003. Smad3 mediates transforming growth factor-β-induced α-smooth muscle actin expression. *Am. J. Respir. Cell. Mol. Biol.* 29: 397–404.
58. Rosenkilde, M. M., and T. W. Schwartz. 2004. The chemokine system–a major regulator of angiogenesis in health and disease. *APMIS* 112: 481–495.
59. Bernardini, G., D. Ribatti, G. Spinetti, L. Morbidelli, M. Ziche, A. Santoni, M. C. Capogrossi, and M. Napolitano. 2003. Analysis of the role of chemokines in angiogenesis. *J. Immunol. Methods* 273: 83–101.
60. Distler, J. H., A. Hirth, M. Kurowska-Stolarska, R. E. Gay, S. Gay, and O. Distler. 2003. Angiogenic and angiostatic factors in the molecular control of angiogenesis. *Q. J. Nucl. Med.* 47: 149–161.
61. Sunderkotter, C., K. Steinbrink, M. Goebeler, R. Bhardwaj, and C. Sorg. 1994. Macrophages and angiogenesis. *J. Leukocyte Biol.* 55: 410–422.
62. Swift, M. E., H. K. Kleinman, and L. A. DiPietro. 1999. Impaired wound repair and delayed angiogenesis in aged mice. *Lab. Invest.* 79: 1479–1487.
63. Frank, S., M. Madlener, and S. Werner. 1996. Transforming growth factors β1, β2, and β3 and their receptors are differentially regulated during normal and impaired wound healing. *J. Biol. Chem.* 271: 10188–10193.
64. Ozawa, K., T. Kondo, O. Hori, Y. Kitao, D. M. Stern, W. Eisenmenger, S. Ogawa, and T. Ohshima. 2001. Expression of the oxygen-regulated protein ORP150 accelerates wound healing by modulating intracellular VEGF transport. *J. Clin. Invest.* 108: 41–50.
65. Jeon, S. H., B. C. Chae, H. A. Kim, G. Y. Seo, D. W. Seo, G. T. Chun, N. S. Kim, S. W. Yie, W. H. Byeon, S. H. Eom, et al. 2007. Mechanisms underlying TGF-β1-induced expression of VEGF and Flk-1 in mouse macrophages and their implications for angiogenesis. *J. Leukocyte Biol.* 81: 557–566.
66. Nakagawa, T., J. H. Li, G. Garcia, W. Mu, E. Piek, E. P. Bottinger, Y. Chen, H. J. Zhu, D. H. Kang, G. F. Schreiner, et al. 2004. TGF-β induces proangiogenic and antiangiogenic factors via parallel but distinct Smad pathways. *Kidney Int.* 66: 605–613.
67. Nakagawa, T., H. Y. Lan, H. J. Zhu, D. H. Kang, G. F. Schreiner, and R. J. Johnson. 2004. Differential regulation of VEGF by TGF-β and hypoxia in rat proximal tubular cells. *Am. J. Physiol.* 287: F658–F664.
68. Benckert, C., S. Jonas, T. Cramer, Z. Von Marschall, G. Schafer, M. Peters, K. Wagner, C. Radke, B. Wiedenmann, P. Neuhaus, et al. 2003. Transforming growth factor β 1 stimulates vascular endothelial growth factor gene transcription in human cholangiocellular carcinoma cells. *Cancer Res.* 63: 1083–1092.